A CPW-Fed UWB-MIMO Antenna with High Isolation and Dual Band-Notched Characteristic

Jian-Yong Zhou[1, 2], Yan-Fei Wang[2], Jia-Ming Xu[3], and Cheng-Zhu Du[3, *]

Abstract—A coplanar waveguide (CPW) fed multiple-input multiple-output (MIMO) ultra-wideband (UWB) antenna with high isolation and dual band-notched characteristic is proposed. The antenna consists of two orthogonal circle patches. An annular slot and a rectangular slot are added on the patches to produce two notched bands. High isolation is successfully acquired by adopting a double Y-shaped branch between the two radiation elements. By cutting the fractional substrate, the antenna size has been reduced by 31.4 percent. The measured results show that the working bandwidth of the antenna covers 2.36–12 GHz, and at the same time, the notched bands cover 3.37 GHz–3.98 GHz and 4.71 GHz–5.51 GHz. The isolation is better than 21 dB. The paper also studies the radiation pattern, peak gain, and envelope correlation coefficient (ECC) of the UWB MIMO antenna.

1. INTRODUCTION

Ultra-wideband (UWB) technology possesses great merits including high data rate, low cost, and easy fabrication. Many scholars are keen on UWB antennas with band-notched characteristics [1, 2]. Using the spatial multiplexing gain and spatial diversity gain of multiple-input multiple-output (MIMO) technology can increase the transmission rate and anti-interference of antennas. However, when radiation patches are printed on the same substrate, there will be mutual coupling between antennas. Scholars have proposed many different decoupling methods in the literature. Tiwari et al. proposed a method in his article that he used neutral lines to offset the coupling current on the radiation patch [3]. Different shape and size branches are added between the radiators of an antenna [4, 5], and the function of the branches is to reduce the current flowing from port 1 to port 2 and achieve decoupling effect.

UWB operating frequency covers a wide range, including WiMAX (3.4 GHz–3.69 GHz) and WLAN (5.15 GHz–5.35 GHz) systems. In order to avoid mutual interference, some UWB MIMO antennas with band-notch characteristics have been proposed [6–14].

A microstrip-fed UWB MIMO antenna with a cross-shaped stub is presented in [15], and the cross-shaped stub is used to reduces mutual coupling between monopoles. Finally, the working bandwidth of this antenna is 2.97–13.8 GHz, and the isolation S_{21} is less than -15 dB. A coaxially fed UWB MIMO antenna with a reflector to enhance isolation is designed in [16], and the port isolation of the designed antenna is less than -20 dB in the range of 3.1–10.6 GHz. However, the antenna mentioned in the above paper does not realize the function of notch. In [17], a novel compact MIMO antenna system with dual polarizations based on microstrip feed is proposed, and the measured results show that the proposed antenna has a bandwidth ranging from 3 to 12 GHz with port isolation $S_{21} < -15$ dB in work band, but it only achieves band rejection at WLAN system. In [18, 19], a UWB-MIMO antenna with dual notch characteristics is realized by the CPW feeding method, and the isolation degree is more than

15 dB. A two-port UWB-MIMO antenna with dual band-notched characteristics is presented in [20, 21]. A UWB MIMO slot antenna with Minkowski fractal shaped isolators for isolation enhancement is designed in [22]. In [23], a planar UWB MIMO-diversity antenna with dual notches is proposed, and the proposed antenna is based on Quasi Self Complementary (QSC) method to give wide impedance bandwidth from 2.4 GHz to more than 12 GHz.

In this paper, a UWB MIMO antenna with high isolation and dual band-notched characteristics based on CPW feed is designed. The antenna consists of two orthogonal circular elements fed by CPW. By etching two slots of different sizes in the radiators, the antenna generates dual notched bands for UWB applications. The working band is from 2.36 to 12 GHz except WiMAX and WLAN systems. The measured results show that the isolation of the antenna is more than -21 dB in the range of 2–12 GHz. Moreover, the CPW feed is easier to integrate or conform to the circuit or equipment, and can reduce dispersion efficiency. The detailed process design and structural analysis of the antenna are given below.

2. ANTENNA DESIGN AND CONFIGURATIONS

This design is based on ANSOFT HFSS 15 to simulate and optimize the structure and parameters of the antenna. The proposed antenna is shown in Figure 1. MIMO antenna is printed on FR4 with dielectric constant of 4.4 and thickness of 0.8 mm. The radiation element uses a circular patch for covering UWB system. The rectangular slot and annular slot produce different frequency band-notches. High isolation is achieved by loading a branch between two radiators. Through simulation and optimization, the final antenna size is shown: $L = 50$ mm, $L_1 = 8$ mm, $L_2 = 22$ mm, $L_d = 9$ mm, $S_1 = 36$ mm, $S_2 = 16$ mm, $S_3 = 14.5$ mm, $S_4 = 5.6$ mm, $L_{Z1} = 13.6$ mm, $L_{Z2} = 3$ mm, $W = 50$ mm, $W_1 = 14.5$ mm, $W_2 = 5.6$ mm, $W_f = 0.2$ mm, $W_d = 3$ mm, $W_{Z1} = 5$ mm, $W_{Z2} = 0.6$ mm, $R_0 = 8.7$ mm, $R_1 = 3$ mm, $a_1 = 60°$, $a_2 = 70°$.
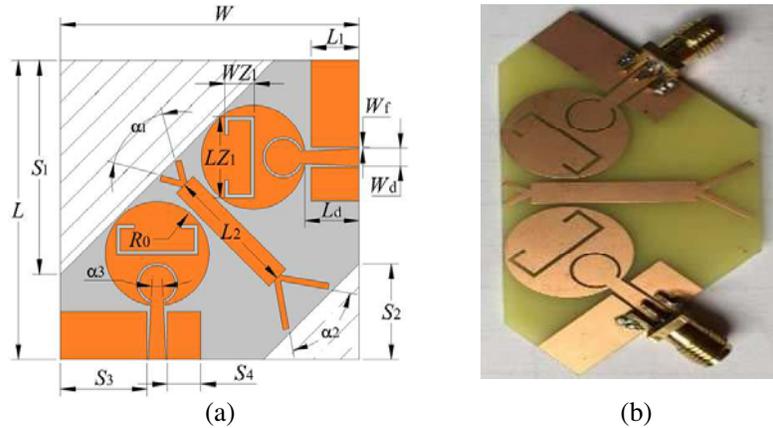
Figure 1. Proposed antenna. (a) Configuration; (b) photograph.

3. ANALYSIS OF THE PROPOSED ANTENNA

In this section, the effects of different structures on antenna S_{11} and S_{21} are analyzed, and the analysis of S-parameters can clearly and intuitively understand the function of various antenna structures and the design process of loading notches are also explained.

3.1. Structure Analysis of the Antenna

As shown in Figure 2, the defective ground structure (DGS) is used to reduce the direct flow of current from one port to another. In order to understand the influence of DGS on antenna performance, the relationship between ground length S_4 and antenna S parameters is given in Figure 3. When the length S_4 is 32 mm, the ground of the two radiation elements will be directly connected. As the length
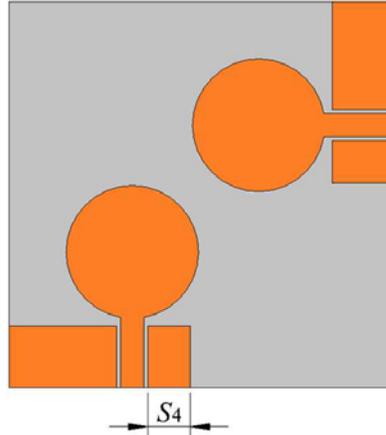
Figure 2. The schematic diagram of antenna substrate with DGS.
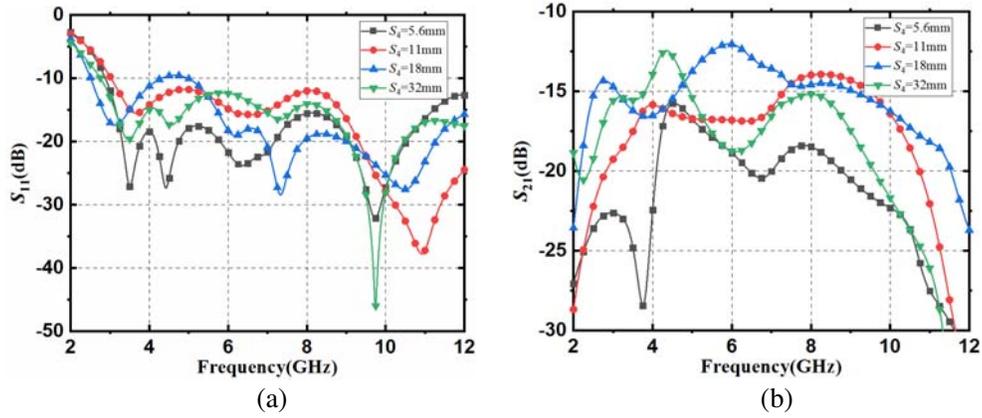
Figure 3. The relationship between floor length S_4 and antenna S-parameters. (a) S_{11}; (b) S_{21}.

S_4 decreases, the ground distance between the antenna radiating elements increases, and the coupling current on the coplanar ground decreases, so S_{11} is reduced from the highest -9.5 dB to -15.9 dB, and S_{21} is also significantly improved. When S_4 is 5.6 mm, the port isolation is less than -15 dB, which meets the design requirements of the MIMO antenna.

As shown in Figure 4, by cutting off the two isosceles triangles on the substrate, the size of the antenna has been reduced by 31%. Figure 5 shows the comparisons of S-parameters with and without cut of the antenna. It can be seen from the figure that cutting the substrate makes little change on S_{11}, while for port isolation, it has the obvious effect on optimizing isolation, and S_{21} of the antenna in the range of 4.7–5.9 GHz is less than -20 dB.

The design process of the antenna structure is shown in Figure 6. By adding two slots, the antenna has the filtering function. The principle of forming a notch by slotting is that the current directions on both sides of the slot are opposite, so the distribution currents cancel each other. The length of slot is generally $\frac{\lambda}{2}$ or $\frac{\lambda}{4}$ as follows:

$$L_1 = \frac{C}{2f_{center} \cdot \sqrt{\varepsilon_{eff}}} \tag{1}$$

$$L_2 = \frac{C}{4f_{center} \cdot \sqrt{\varepsilon_{eff}}} \tag{2}$$

$$\varepsilon_{eff} = \frac{\varepsilon_r + 1}{2} \tag{3}$$
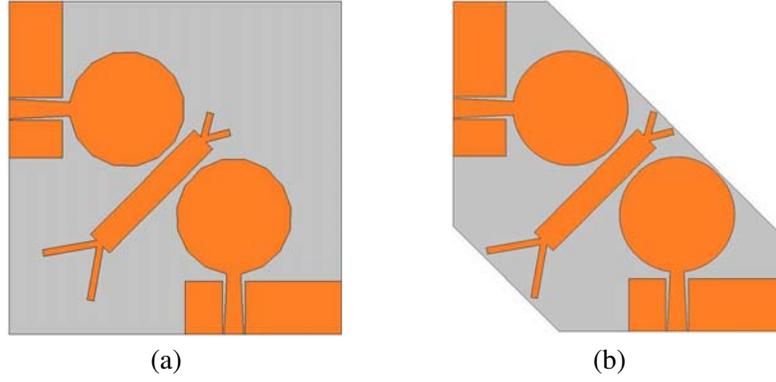
Figure 4. The schematic diagram of antenna substrate without and with cut. (a) Substrate without cut; (b) substrate with cut.
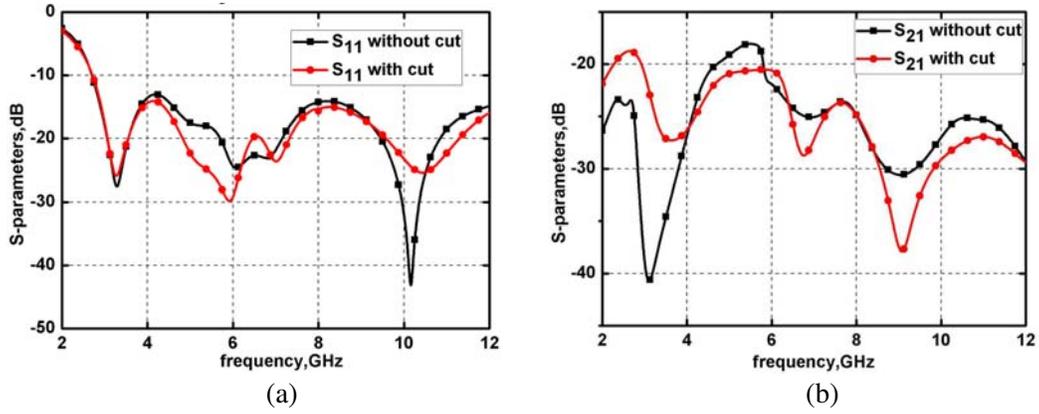
Figure 5. The comparison of S-parameters without and with substrate cut. (a) S_{11}; (b) S_{21}.
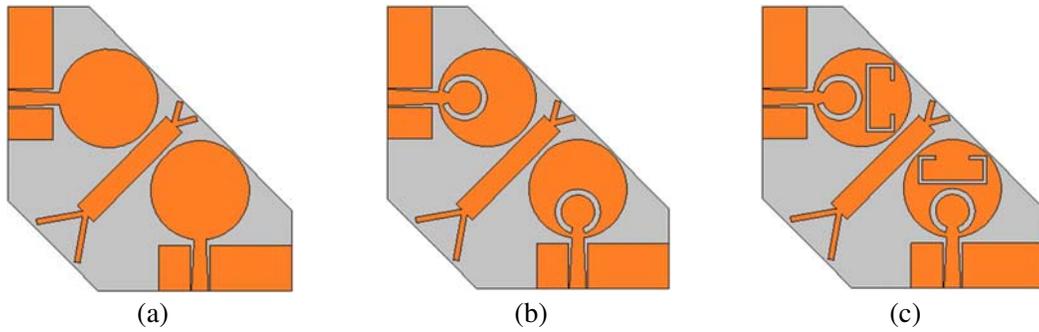
Figure 6. The design process of the antenna structure. (a) Without slots; (b) with annular slot; (c) with annular and rectangle slots.

where C denotes the speed of light, f_{center} the center frequency corresponding to the notched band, and ε_r the relative dielectric constant of the medium.

Figure 7 shows the influence of different slots on S-parameter. From the figure, it can be seen that when the annular slot is added, a notch ($S_{11} > -10$ dB) frequency range of 4.77–5.61 GHz is generated, and due to the corrosion of annular and rectangular slots on the radiation patch, S_{11} are higher than -10 dB in 3.28–3.96 GHz and 4.77–5.61 GHz bands corresponding to WiMAX and WLAN systems.

Figure 8 shows the schematic diagram with and without a branch, and its effect on S-parameter is
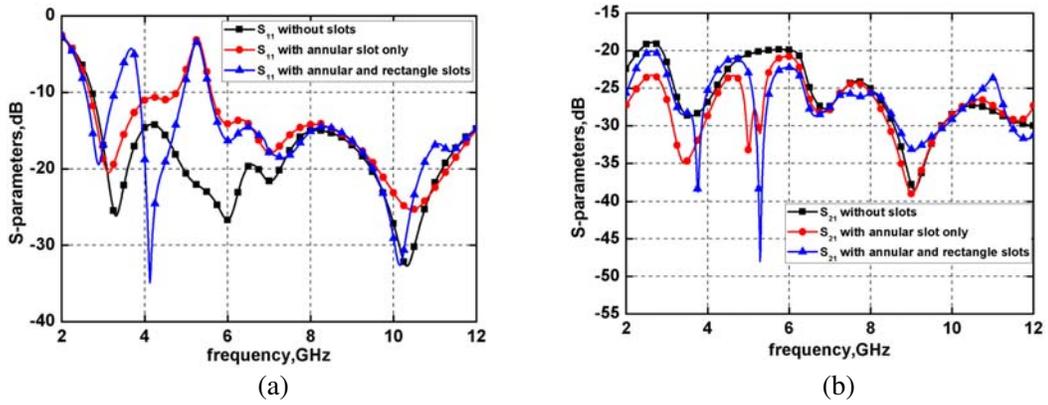
Figure 7. The influence of different slots on S-parameter. (a) S_{11}; (b) S_{21}.
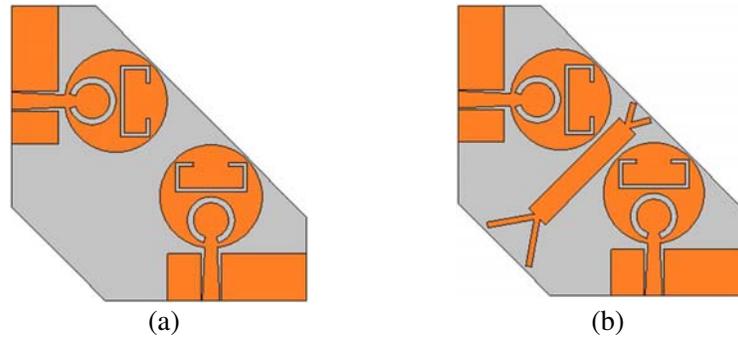
Figure 8. The schematic diagram with and without branch. (a) Without branch; (b) with branch.
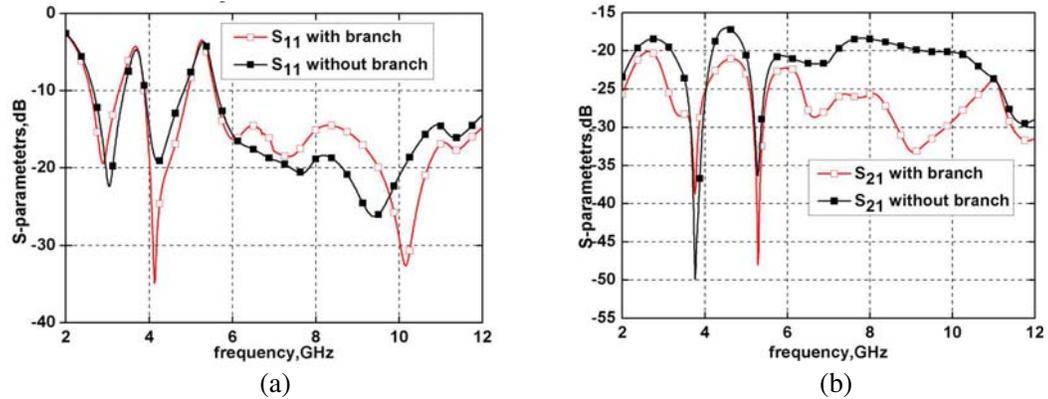
Figure 9. The influence of branch on S-parameter. (a) S_{11}; (b) S_{21}.

shown in Figure 9. It can be clearly seen that S_{21} of the antenna decreases by loading a branch at least 2 dB in the range of 2–12 GHz, and especially within 6–12 GHz, the decoupling effect is more obvious.

3.2. Current Distribution of the Antenna

Figure 10 shows the current distribution of the MIMO antenna with and without a branch. The double Y-shaped branch is added between two antenna elements to increase port isolation. Antenna element 1 is excited at port 1, and antenna element 2 is excited at port 2. The principle of reducing coupling of

(a) (a)
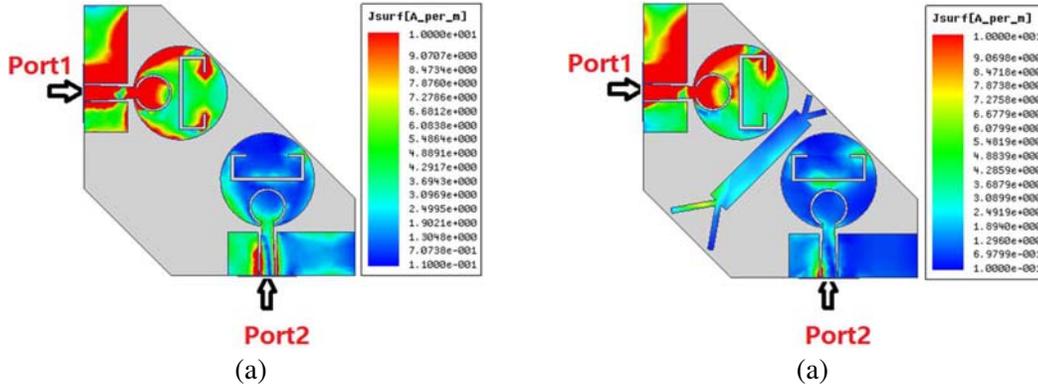
Figure 10. The current distribution of MIMO antenna with and without branch when port 1 is the exciting end and port 2 is connected with 50 Ω load. (a) Without branch; (b) with branch.

two antenna elements is that when antenna element 1 is excited, the two induction currents of antenna element 2 will be generated by antenna element 1 and the double Y-shaped branch. If the phases of two inductive current are opposite, then the two induction currents will cancel each other, and at last the port isolation of the antenna is improved. It can be clearly observed that a large number of coupling currents on the ground of antenna element 2 (the red part shown in the figure is the current concentration area) are significantly reduced by adding the double Y-shaped branch.

Figure 11 shows the current distributions of the notch center frequency at 3.6 GHz and 5.3 GHz. It can be seen that when the antenna operates at these two frequencies, a large amount of energy is concentrated on the circular slot and rectangular slot (the red part shown in the figure is the current concentration area). The energy cannot be radiated, thus forming a gap.

(a) (b)
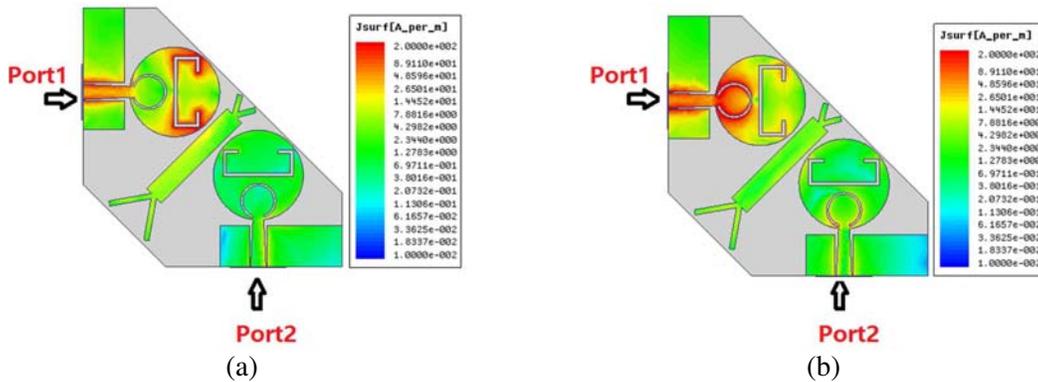
Figure 11. The current distribution of the antenna when port 1 is the exciting end and port 2 is connected with 50 Ω load. (a) At 3.6 GHz; (b) at 5.3 GHz.

4. RESULTS AND DISCUSSION

4.1. Measured and Simulated on *S*-Parameters

The return loss and isolation of antenna are measured by Agilent E8363c vector network analyzer. Figure 12 shows a comparison of *S*-parameters between simulation and measurement. The measured curve is slightly different from the simulation curve at 6–12 GHz because of the processing accuracy and the possible deviation of SMA joint welding, but it is always less than −10 dB. The measured notch band covers 3.37 GHz–3.98 GHz and 4.71 GHz–5.51 GHz corresponding to WiMAX and WLAN systems. The isolation S_{21} is less than −21 dB in the UWB range.

The measured radiation patterns of the proposed antenna at 4.2 GHz and 10.6 GHz in H plane and E plane are shown in Figure 13. In the H plane, the radiation patterns are shown as nearly omnidirectional patterns. In the E-plane it is bidirectional radiation model. Because the symmetry of the coplanar ground is destroyed by cutting off part of it, it appears deformed in the high frequency pattern, but it does not affect the antenna radiation performance.

(a)

(b)
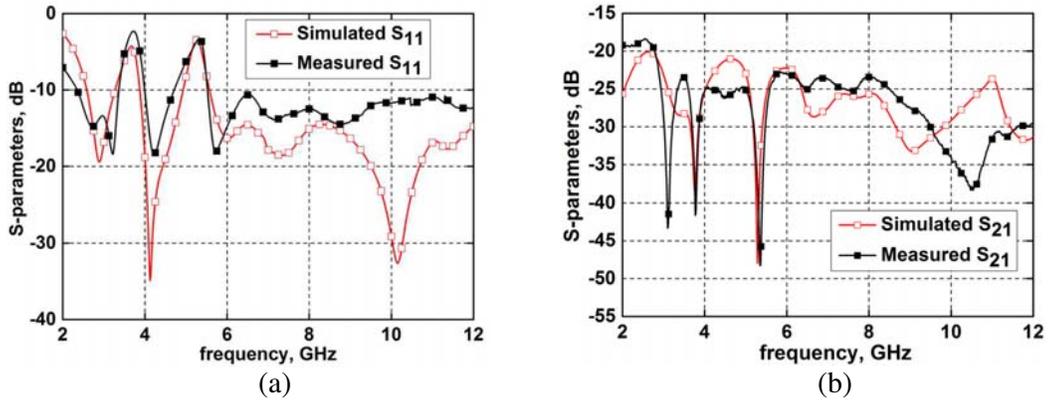
Figure 12. The comparison of S-parameters between simulation and measurement. (a) S_{11}; (b) S_{21}.

E-plane (a) H-plane
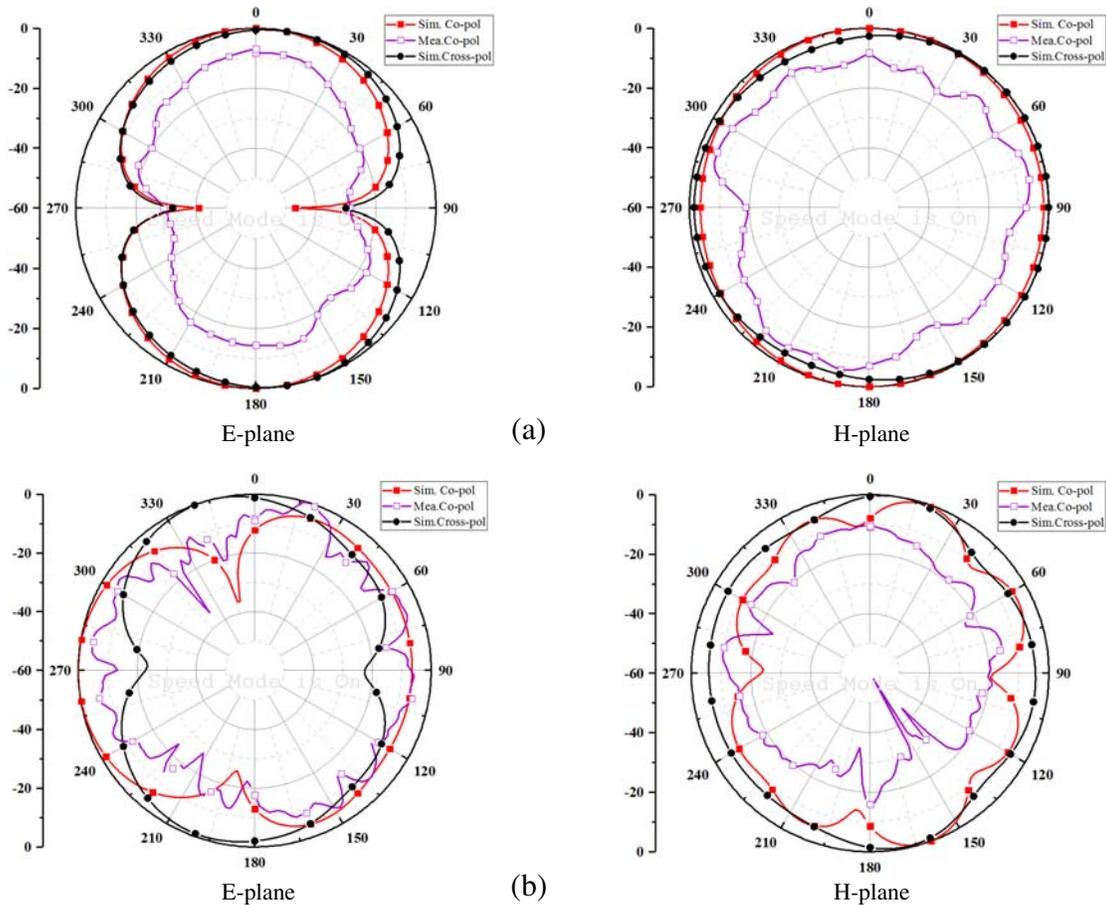
E-plane (b) H-plane

Figure 13. E-plane and H-plane radiation patterns of the purposed MIMO antenna at (a) 4.2 GHz and (b) 10.6 GHz.

4.2. ECC Curve

The envelope correlation coefficient (ECC) represents the correlation of measuring the amplitude of MIMO antenna signal. The calculation formula is shown in Eq. (4) [9] below. Figure 14 shows the comparison of simulated and measured ECCs of MIMO antenna. It can be seen that the ECC value is less than 0.04, which meets the design criterion.

$$ECC = \left| \frac{S_{11}^* S_{12} + S_{21}^* S_{22}}{\left(\sqrt{1 - |S_{11}|^2 - |S_{21}|^2} \right) \cdot \left(\sqrt{1 - |S_{22}|^2 - |S_{12}|^2} \right)} \right| \tag{4}$$

4.3. Diversity Gain

Diversity gain (DG) can evaluate MIMO antenna isolation performance. The diversity gain is calculated as follows:

$$DG = 10\sqrt{1 - (ECC)^2} \tag{5}$$

The value of DG is associated with ECC. Generally, the value of the required diversity gain on engineering is greater than 9.9. It can be seen from Figure 15 that the simulated and measured DG values in the operating frequency band are much greater than 9.9, which meets the engineering standard.
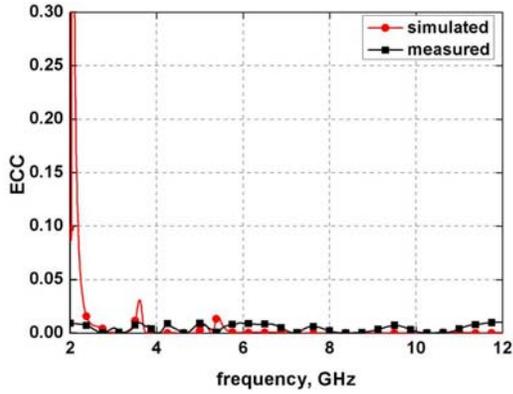
Figure 14. The comparison of simulated and measured ECC of MIMO antenna.
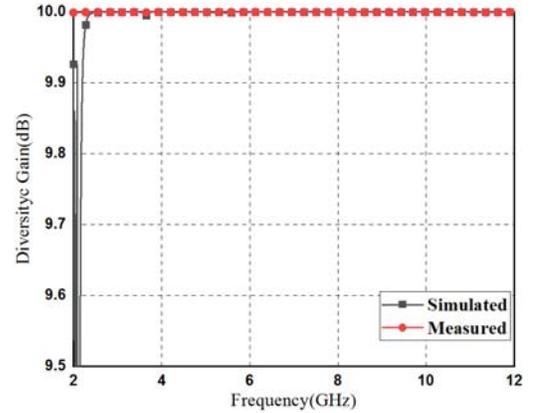
Figure 15. DG of the purposed antenna.
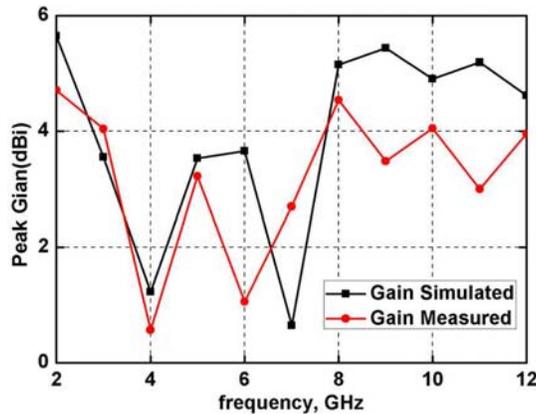
Figure 16. The comparison of simulated and measured gains of proposed antenna.

4.4. Gain

Gain is used to measure the ability of an antenna to receive and transmit signals. Figure 16 shows the comparison of simulated and measured gains of the proposed antenna. The measured gain from 2–12 GHz varies between 2.13 and 4.71 dB, excluding the gain in the notch bands.

5. COMPARISON WITH OTHER WORKS

Table 1 shows the comparison between the proposed antenna and previously reported UWB MIMO antennas in terms of antenna feeding method, bandwidth, isolation, the number of notches, and ECC value. Compared with the antennas designed before, the CPW-fed antenna designed in this paper achieves high isolation, low ECC, and dual band-notched characteristics. It can be etched on a limited patch to achieve notch function, which makes UWB-MIMO antenna more widely used.

Table 1. Comparison between the proposed antenna and previously reported UWB MIMO antennas.

Refer-ences	No. of Ports	Effective area (mm^2)	Thickness (mm)	Feeding method	Bandwidth (GHz)	Isolation (dB)	Bands notched	ECC	DG	Isolation technique
[15]	2	625	1.6	Microstrip	2.97–13.8 (129%)	< -15	0	< 0.05	9.97	Stubs
[16]	2	750	1.6	Coaxial	3.1–10.6 (97%)	< -20	0	< 0.16	-	Slot
[17]	2	1225	1	Microstrip	3–12 (120%)	< -15	1	< 0.5	-	Stubs
[18]	2	881	1.6	CPW	3.05–13.5 (126%)	< -15	2	< 0.1	9.96	Slot/ neutral lines
[19]	2	1600	0.8	CPW	3.4–12 (111%)	< -15	2	< 0.5	-	Slot
[20]	2	1472	1.6	CPW	3.1–16 (136%)	< -15	2	< 0.15	-	Slot
[21]	2	570	0.8	Microstrip	3.1–1.06 102%)	< -18	2	< 0.25	-	Stubs
[22]	2	2116	0.8	CPW	3.1–12 (117%)	< -17	1	< 0.02	-	Orthogonal/ Stubs/ Minkowski
[23]	4	1702	1.5	Microstrip	2.5–12 (131%)	< -20	2	< 0.005	9.96	Orthogonal
This work	2	1724	0.8	CPW	2.36–12 (134%)	< -21	2	< 0.04	9.99	Orthogonal/ Stubs/ DGS

6. CONCLUSION

In this paper, a CPW-fed UWB-MIMO antenna with high isolation and dual band-notched characteristics has been designed. The proposed antenna has a work bandwidth from 2.36 to 12 GHz (VSWR < 2.134%), excepting two notched bands: 3.37–3.98 GHz and 4.71–5.51 GHz which cover WiMAX and WLAN systems. By loading double Y-shaped branch between the two radiation elements, high isolation of better than 21 dB is achieved. Moreover, the peak gain is 4.71 dB, and the ECC is less than 0.04 over the entire UWB operational bandwidth. Therefore, the proposed MIMO antenna is suitable for UWB systems.

REFERENCES

1. Sultan, K. S., O. M. A. Dardeer, and H. A. Mohamed, "Design of compact dual notched self-complementary UWB antenna," *Open Journal of Antennas and Propagation*, Vol. 05, No. 03, 99–109, 2017.

2. Xu, J., C. Du, G. Jin, K. Li, W. Zheng, and Z. Zhao, "A coplanar feed quad-band notched UWB antenna," *2019 International Workshop on Electromagnetics: Applications and Student Innovation Competition (iWEM)*, 1–2, Qingdao, China, 2019.

3. Tiwari, R. N., P. Singh, B. K. Kanaujia, and K. Srivastava. "Neutralization technique based two and four port high isolation MIMO antennas for UWB communication," *AEUE - International Journal of Electronics and Communications*, Vol. 110, 2019.

4. Wu, L. and Y. Q. Xia. "Compact UWB-MIMO antenna with quadband-notched characteristic," *International Journal of Microwave and Wireless Technologies*, Vol. 9, No. 5, 1147–1153, 2017.

5. Ibrahim, A., M. Abdalla, and Z. Hu, "Design of a compact MIMO antenna with asymmetric coplanar strip-fed for UWB applications," *Microwave and Optical Technology Letters*, Vol. 59, No. 1, 31–36, 2017.

6. Yang, Z., F. Li, and F. Li, "A compact slot MIMO antenna with band-notched characteristic for UWB application," *2018 International Conference on Microwave and Millimeter Wave Technology (ICMMT)*, 1–3, 2018.

7. Li, Z., C. Yin, and X. Zhu, "Compact UWB MIMO Vivaldi antenna with dual band-notched characteristics," *IEEE Access*, Vol. 7, No. 99, 38696–38701, 2019.

8. He, Z., Z. Yang, and J. Lv, "Design of a novel band-notched antenna for UWB MIMO communication system," *2018 International Conference on Microwave and Millimeter Wave Technology (ICMMT)*, 1–3, 2018.

9. Gautam, A., S. Yadav, and K. Rambabu, "Design of ultra-compact UWB antenna with band-notched characteristics for MIMO applications," *IET Microwaves, Antennas & Propagation*, Vol. 12, No. 12, 1895–1900, 2018.

10. Zhang, J.-Y., W.-P. Tian, Y.-L. Luo, and F. Zhang, "ACS-fed UWB-MIMO antenna with shared radiator," *Electronics Letters*, Vol. 51, No. 17, 1301–1302, 2015.

11. Hasan, M., S. Chu, and S. Bashir, "A DGS monopole antenna loaded with U-shape stub for UWB MIMO applications," *Microwave and Optical Technology Letters*, Vol. 61, No. 9, 2141–2149, 2019.

12. He, Z., Z. Yang, and J. Lv, "Design of a novel band-notched antenna for UWB MIMO Communication System," *2018 International Conference on Microwave and Millimeter Wave Technology (ICMMT)*, 1–3, 2018.

13. Li, J., D. Wu, Y. Wu, and G. Zhang, "Dual band-notched UWB MIMO antenna," *2015 IEEE 4th Asia-Pacific Conference on Antennas and Propagation (APCAP)*, 25–26, Kuta, 2015.

14. Hasan, M., P. Singh, and M. Nadeem, "Omnidirectional UWB antenna loaded with rectangular loop for band notch characteristics," *2019 6th International Conference on Signal Processing and Integrated Networks (SPIN)*, 425–429, 2019.

15. Singh, H. and S. Tripathi, "Compact UWB MIMO antenna with cross-shaped unconnected ground stub using characteristic mode analysis," *Microwave and Optical Technology Letters*, Vol. 61, No. 7, 1874–1881, 2019.

16. Roshna, T. K., U. Deepak, V. R. Sajitha, K. Vasudevan, and P. Mohanan, "A compact UWB MIMO antenna with reflector to enhance isolation," *IEEE Transactions on Antennas and Propagation*, Vol. 63, No. 4, 1873–1877, April 2015.

17. Zhu, J., S. Li, B. Feng, L. Deng, and S. Yin, "Compact dual-polarized UWB quasi-self-complementary MIMO/diversity antenna with band-rejection capability," *IEEE Antennas and Wireless Propagation Letters*, Vol. 15, 905–908, 2016.

18. Banerjee, J., R. Ghatak, and A. Karmakar, "A compact planar UWB MIMO diversity antenna with Hilbert fractal neutralization line for isolation improvement and dual band notch characteristics," *2018 Emerging Trends in Electronic Devices and Computational Techniques (EDCT)*, 1–6, Kolkata, 2018.

19. Zhu, J., B. Feng, B. Peng, et al., "Compact CPW UWB diversity slot antenna with dual band-notched characteristics," *Microwave and Optical Technology Letters*, Vol. 58, No. 4, 989–994, 2016.

20. Zhang, J., L. Wang, and W. Zhang, "A novel dual band-notched CPW-fed UWB MIMO antenna with mutual coupling reduction characteristics," *Progress In Electromagnetics Research Letters*, Vol. 90, 21–28, 2020.

21. Kumar, A., A. Q. Ansari, B. K. Kanaujia, et al., "An ultra-compact two-port UWB-MIMO antenna with dual band-notched characteristics," Vol. 114, 152997, 2019.

22. Debnath, P., A. Karmakar, A. Sah, and S. Huda, "UWB MIMO slot antenna with minkowski fractal shaped isolators for isolation enhancement," *Progress In Electromagnetics Research M*, Vol. 75, 69–78, 2018.

23. Sultan, K. S. and H. H. Abdullah, "Planar UWB MIMO-diversity antenna with dual notch characteristics," *Progress In Electromagnetics Research C*, Vol. 93, 119–129, 2019.